System code analysis of accumulator nitrogen discharge during LOCA experiment at PWR PACTEL test facility

Kauppinen Otso-Pekka, Kouhia Virpi, Riikonen Vesa, Hyvärinen Juhani

DOI: 10.1016/j.nucengdes.2019.110288

Elsevier Editorial System(tm) for Nuclear Engineering and Design

Manuscript Draft

Manuscript Number: NED-D-19-00102R1

Title: System code analysis of accumulator nitrogen discharge during LOCA experiment at PWR PACTEL test facility

Article Type: Full Length Article

Keywords: PWR PACTEL; LOCA; nitrogen; accumulator; TRACE; APROS

Corresponding Author: Mr. Otso-Pekka Kauppinen,

Corresponding Author's Institution: LUT University

First Author: Otso-Pekka Kauppinen

Order of Authors: Otso-Pekka Kauppinen; Virpi Kouhia; Vesa Riikonen; Juhani Hyvärinen

Abstract: The hydroaccumulators in pressurized water reactors can inject nitrogen into the reactor system. In the primary system, nitrogen affects core cooling and accident management, both adversely and beneficially. The PWR PACTEL experiment NCG-13 have shown that during a hot leg SB LOCA, nitrogen in the primary side can block the primary to secondary heat transfer and thereby prevent the primary depressurization to the point needed for the long-term accident management. This paper presents the APROS and TRACE calculations of the PWR PACTEL NCG-13 experiment. Both codes calculate the transient progression and the timing of the main events satisfactorily, once the suitable options are selected and adjustments made. There is, however, one big discrepancy between the code simulations and the experiment: in the simulations, much more nitrogen is needed to get qualitatively the same behaviour. The difference is a factor of 2.5 by mass for stopping the depressurization and 4-6 to cause a core heat-up. This is of concern regarding the confidence in the codes, as the simulations underestimate the adverse effect of nitrogen on the core coolability.

HIGHLIGHTS:

- Codes predict the transient behaviour and timing of the main events satisfactory
- In the simulations, nitrogen stops the primary side depressurization
- Amount of released nitrogen is larger in the simulations than in the experiment

*Title Page

System code analysis of accumulator nitrogen discharge during LOCA experiment at PWR PACTEL test facility

AUTHORS:

Otso-Pekka Kauppinen[a], Virpi Kouhia[a], Vesa Riikonen[a], Juhani Hyvärinen[a]

AFFILIATION:

[a] LUT University, LUT School of Energy Systems, Nuclear Engineering, P.O. BOX 20, FI-53851 Lappeenranta, Finland

E-MAIL ADDRESSES:

otso-pekka.kauppinen@lut.fi (Otso-Pekka Kauppinen), virpi.kouhia@lut.fi (Virpi Kouhia), vesa.riikonen@lut.fi (Vesa Riikonen), juhani.hyvarinen@lut.fi (Juhani Hyvärinen)

CORRESPONDING AUTHOR:

* Otso-Pekka Kauppinen, LUT University, LUT School of Energy Systems, Nuclear Engineering, P.O. BOX 20, FI-53851 Lappeenranta, Finland, +358 40 152 9448

KEYWORDS:

PWR PACTEL, LOCA, nitrogen, accumulator, TRACE, APROS

System code analysis of accumulator nitrogen discharge during LOCA experiment at PWR PACTEL test facility

Abstract

The hydroaccumulators in pressurized water reactors can inject nitrogen into the reactor system. In the primary system, nitrogen affects core cooling and accident management, both adversely and beneficially. The PWR PACTEL experiment NCG-13 have shown that during a hot leg SB LOCA, nitrogen in the primary side can block the primary to secondary heat transfer and thereby prevent the primary depressurization to the point needed for the long-term accident management. This paper presents the APROS and TRACE calculations of the PWR PACTEL NCG-13 experiment. Both codes calculate the transient progression and the timing of the main events satisfactorily, once the suitable options are selected and adjustments made. There is, however, one big discrepancy between the code simulations and the experiment: in the simulations, much more nitrogen is needed to get qualitatively the same behaviour. The difference is a factor of 2.5 by mass for stopping the depressurization and 4-6 to cause a core heat-up. This is of concern regarding the confidence in the codes, as the simulations underestimate the adverse effect of nitrogen on the core coolability.

Keywords: PWR PACTEL, LOCA, nitrogen, accumulator, TRACE, APROS

1. Introduction

The presence of non-condensable gases (NCGs) in the primary system of a pressurized water reactor (PWR) can affect the thermal-hydraulic behaviour of the reactor coolant system in several ways (Kral et al., 2015). NCGs can have a direct effect on reactor cooling conditions, such as on water distributions and steam condensation.

One of the emergency core cooling systems used in the modern pressure water reactors (PWR) is a hydroaccumulator. The driving force of the accumulator water injection is the pressurized nitrogen volume at the top of the accumulator tank. In a situation when the accumulator is empty of water, remaining nitrogen can enter the reactor system if the flow path is not fully closed after water injection. The nitrogen can affect the pressure levels and distribution of water masses in the pressure vessel. Nitrogen can also migrate to the steam generator tubes and decrease the steam condensation and heat transfer rate from the primary to the secondary side, affecting adversely accident management measures.

At LUT University, the effect of the accumulator nitrogen release on the core cooling during a loss-of-coolant-accident (LOCA) situation was studied with the PWR PACTEL test facility (Riikonen et al., 2016, 2018). The aim of these experiments was to study nitrogen release effects on cooling conditions during LOCA situation and to generate data for the development and validation of the thermal-hydraulic system codes. Among the series of the PWR PACTEL nitrogen experiments, two experiments were set with a break in the hot leg of one loop and the accumulator line connection to the cold leg of the other loop. One experiment was a reference experiment with no nitrogen release whereas the other experiment (NCG-13) included the nitrogen release to the primary system after the water injection ended.

The results of the PWR PACTEL nitrogen experiments with the hot leg break showed a negative impact of the nitrogen release on the core cooling. During the accumulator nitrogen release period the primary side depressurization stopped despite the ongoing secondary side depressurization. The primary side pressure stayed nearly constant until the temperature of the core started to increase. A core heat up occurred at a pressure above or very close to a typical low-pressure safety injection system (LPSI) shut-off head. In the reference experiment without the nitrogen injection, the primary

side pressure followed the secondary side pressure, no heat up occurred, and primary pressure decreased well below LPSI shut-off head.

The accumulator nitrogen release to the primary system during the hot leg break LOCA has been studied earlier with experiments in the BETHSY, PKL and ROSA/LSTF test facilities (Barbier et al., 1996; Schollenberger et al., 2017; Takeda and Ohtsu, 2018). In these experiments, as in the PWR PACTEL nitrogen experiments, the failure of the high-pressure safety injection was assumed and the secondary side depressurization was used as an accident management measure. In the BETHSY experiment, also pressurizer operated-power relief valves (PORVs) were used to depressurize the primary side. In the ROSA/LSTF experiment, the primary system depressurization rate during the secondary side depressurization deteriorated due to the accumulation of nitrogen in the steam generator U-tubes. The primary side pressure stayed above the actuating pressure level of LPSI, causing eventually core heat up, similarly as in the PWR PACTEL NCG-13 experiment.

In the PKL and BETHSY experiment, the energy removal through the break and steam generators (and PORVs in the BETHSY experiment) were adequate to depressurize the primary side below the actuating pressure level of LPSI. In these experiments, the loop seals in some loops were open during the nitrogen inflow. Open loop seals allowed the nitrogen to accumulate in the steam generator U-tubes of these loops. In the other steam generators, the amount of nitrogen was smaller and hence these steam generators were able to remove heat more efficiently and depressurize the primary side.

This paper presents the results of the post-test analysis of the PWR PACTEL nitrogen experiment NCG-13 with the hot leg break. The objective of this analysis is to assess the capability of the used thermal hydraulic system codes and simulation models to predict the effects of nitrogen in the primary side. This analysis gives a closer look of the nitrogen migration in the primary system during the calculations. The codes used in the analysis are the TRAC/RELAP computation engine (TRACE) developed by U.S. NRC and the APROS process simulation software (APROS) developed by Fortum and VTT Technical Research Centre of Finland Ltd.

2. PWR PACTEL facility

PWR PACTEL is a scaled down integral test facility designed to be used in safety studies related to thermal-hydraulics of PWRs with European Pressurized Reactor (EPR) type vertical inverted U-tube steam generators (Kouhia et al., 2012). The facility consists of a pressure vessel model, two loops (broken and intact loop) with vertical steam generators, a pressurizer, and emergency core cooling systems (ECCS) including nitrogen-driven accumulators. The accumulators connect to the primary system in cold leg close to the downcomer nozzle. Fig. 1 presents the general view of the PWR PACTEL test facility and the schematic view of the steam generator.

The pressure vessel of PWR PACTEL comprises a U-tube construction modelling the downcomer, lower plenum, core, and upper plenum. The core rod bundle consists of 144 electrically heated fuel rod elements. The rods are fixed in a triangular grid and located in three parallel channels. The maximum core power is 1 MW, which corresponds roughly to the scaled residual heating power of the EPR reactor. The axial power distribution of the core is a nine-step chopped cosine. The height and volumetric scale of the pressure vessel between PWR PACTEL and EPR is 1:1 and 1:405, respectively.

Both loops simulate one of the reference EPR type primary loops, i.e. the half of the rated EPR capacity is simulated with the PWR PACTEL facility. The hot and cold leg connections to the pressure vessel are at the same elevation and both cold legs consist of loop seals and main circulation pumps. The pressurizer surge line is connected to the hot leg of the broken loop. Both steam generators contain 51 inverted heat exchange U-tubes with the average length of 6.5 m and inner diameter of 16.57 mm. The heat exchange U-tubes are arranged in five main groups with different

lengths. The secondary sides of the steam generators are divided into several volumes (Fig. 1), including the feed water and steam line systems. The height scale of the steam generators and the pressurizer is 1:4 and 1:1.6, respectively. The volumetric scale of the steam generators and the pressurizer is 1:400 and 1:565, respectively. A more detailed description of PWR PACTEL can be found in (Kouhia et al., 2014).

The instrumentation in the facility comprises temperature, pressure, pressure difference, and flow transducers. The power of the core and the heaters in the pressurizer are measured. The location and amount of nitrogen in different parts of the facility is not measured directly. The presence of nitrogen is evaluated indirectly from the available measurement data.

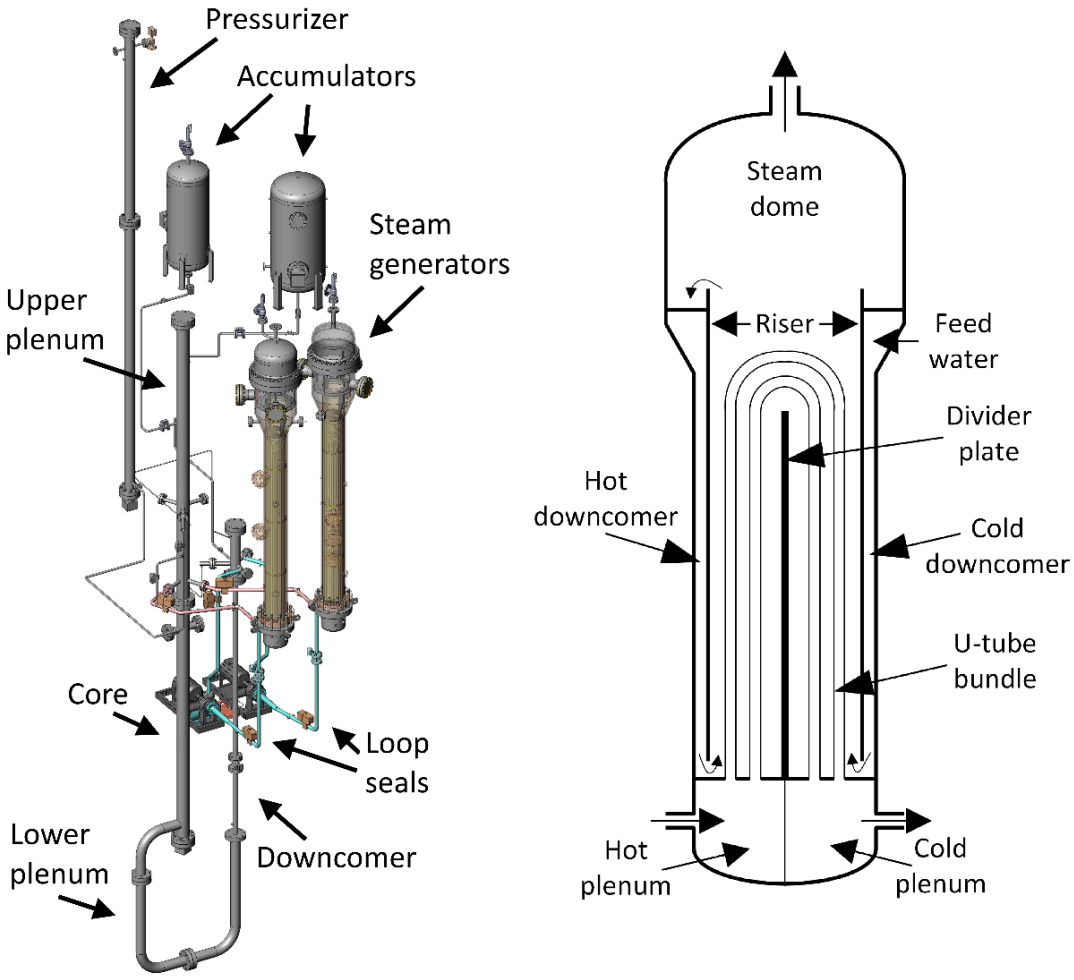

Fig. 1 PWR PACTEL test facility and the schematic view of the PWR PACTEL steam generator.

3. Code nodalizations of the PWR PACTEL facility

The TRACE version 5.0 patch 5 and APROS code version 5.16.05 were used in the post-test simulations of the PWR PACTEL nitrogen experiments. The TRACE system code is developed by the U.S. Nuclear Regulatory Commission (U.S. NRC, 2017) and the APROS system code by the Technical Research Centre of Finland (VTT) and the Finnish power company Fortum (Hänninen and Yli-Joki, 2008; Hänninen, 2009). Both codes use a two-fluid six-equation model based on the one-dimensional mass, momentum, and energy conservation equations. There are differences between the codes, for example, related to the use of the flow regimes, heat transfer and friction correlations, and critical flow models. These factors can plausibly cause differences between the codes in the calculation results.

3.1 Physical modelling of NCGs in the codes

In both codes, NCGs and steam are treated as a gas mixture moving with the same velocity and being at the same temperature (thermal equilibrium). Hence, only single momentum and energy conservation equations are used for the gas mixture. The relative mass concentrations of steam and NCGs are determined by using separate mass conservation equations for each gas component. In the calculations, the dissolved nitrogen in the accumulator water was not considered.

The NCG effect on the steam condensation is taken into account in both codes. In TRACE, the empirical correlation of Sklover and Rodivilin is used in the steam condensation. In APROS, the calculated condensation heat transfer value is multiplied with a correction factor presented by Vierow and Scrock.

The critical flow models are defined in both codes for the single-phase liquid and gas, and two-phase flow. In TRACE, the critical flow for subcooled liquid is calculated using the modified Burnell model. For two-phase, two-component flow in TRACE, the critical mass flux is calculated assuming thermal equilibrium and slip that maximises the mass flux. The critical flow model for single-phase NCG is a special case of the two-phase flow model and is based on isentropic expansion of an ideal gas. In this APROS simulation, the critical mass flow rate is calculated based on the isentropic expansion assumption for liquid, Moody model for two-phase flow and the ideal gas assumption for steam. Consequently, the critical flow models of TRACE and APROS for two-phase flow, with nitrogen present, are physically quite similar to each other.

The location of leak entrance (i.e. above, bottom, or side of the pipe) can affect the quality of the leak flow and consequently the leak mass flow rate if the flow in the horizontal primary side pipe is stratified. TRACE contains a specific offtake model (used in the calculations presented in this paper) to predict an offtake flow quality in this kind of situation. In the APROS simulation, the void fraction of the leak flow is defined according to the void fraction and possible flow stratification in the node in the hot leg where the break line is connected, taking into account the elevation of the break connection. (U.S. NRC, 2017; Kurki et al., 2019)

3.2 PWR PACTEL nodalizations

Fig. 2 presents the TRACE nodalization of the PWR PACTEL facility and Fig. 3 the schematic diagram of the APROS nodalization. Both nodalizations have been utilized and developed within the PWR PACTEL related projects such as with the loop seal clearing experiment case (Kauppinen et al., 2015). Both nodalizations are 1D models including all the main components of the PWR PACTEL facility, such as the pressure vessel, two primary loops with inverted U-tube steam generators, pressurizer, and secondary sides of the steam generators.

In both nodalizations, the core power region in the pressure vessel is modelled with three separate channels and one bypass channel, according to the PWR PACTEL construction. The node lengths in the core are based on the axial power sections of the facility and the axial power distribution in both nodalizations is set according to the facility values. In the TRACE nodalization, the reflood model available in the code is turned on in the core section. Both nodalizations follow the upper plenum, downcomer, and U-shaped lower plenum constructions of the facility. On the top parts of the upper plenum and downcomer, both nodalizations include the narrow diffuser pipe structures and the volumes surrounding the diffusers.

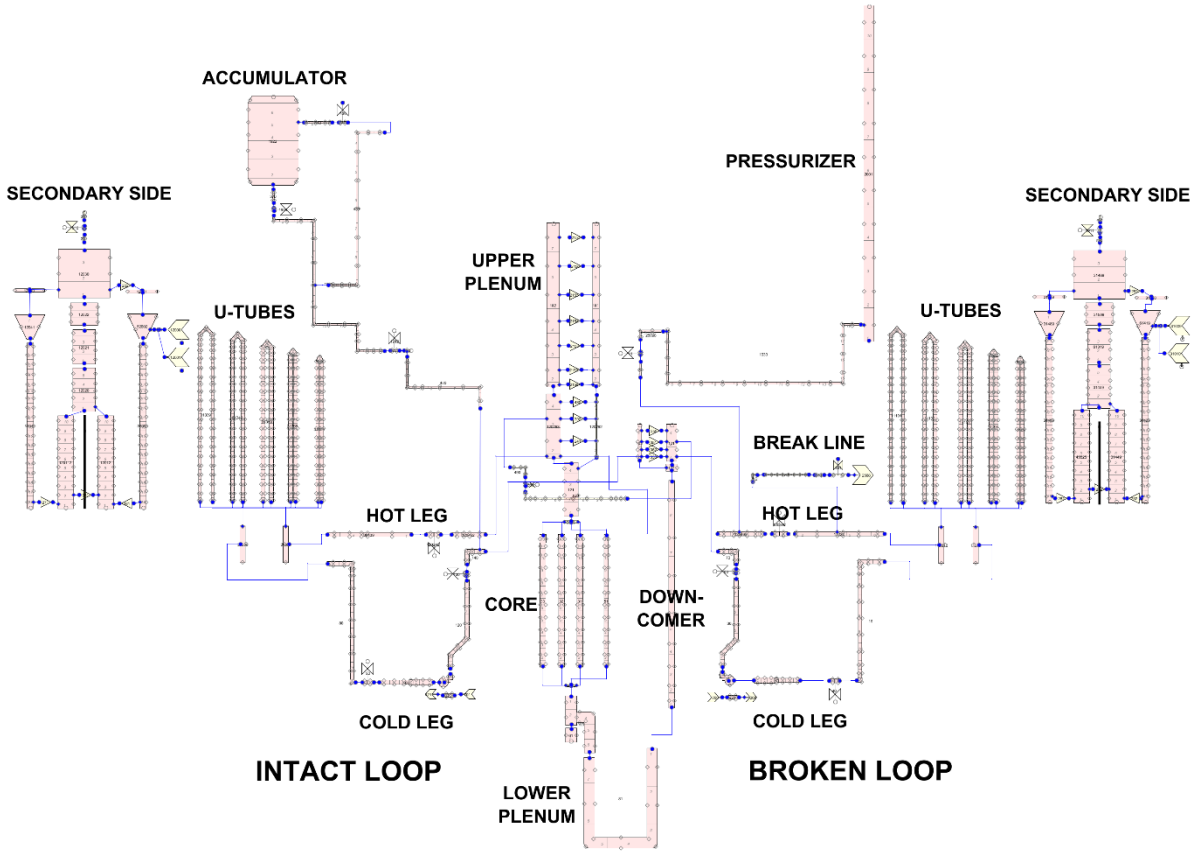

Fig. 2 TRACE nodalization of the PWR PACTEL facility.

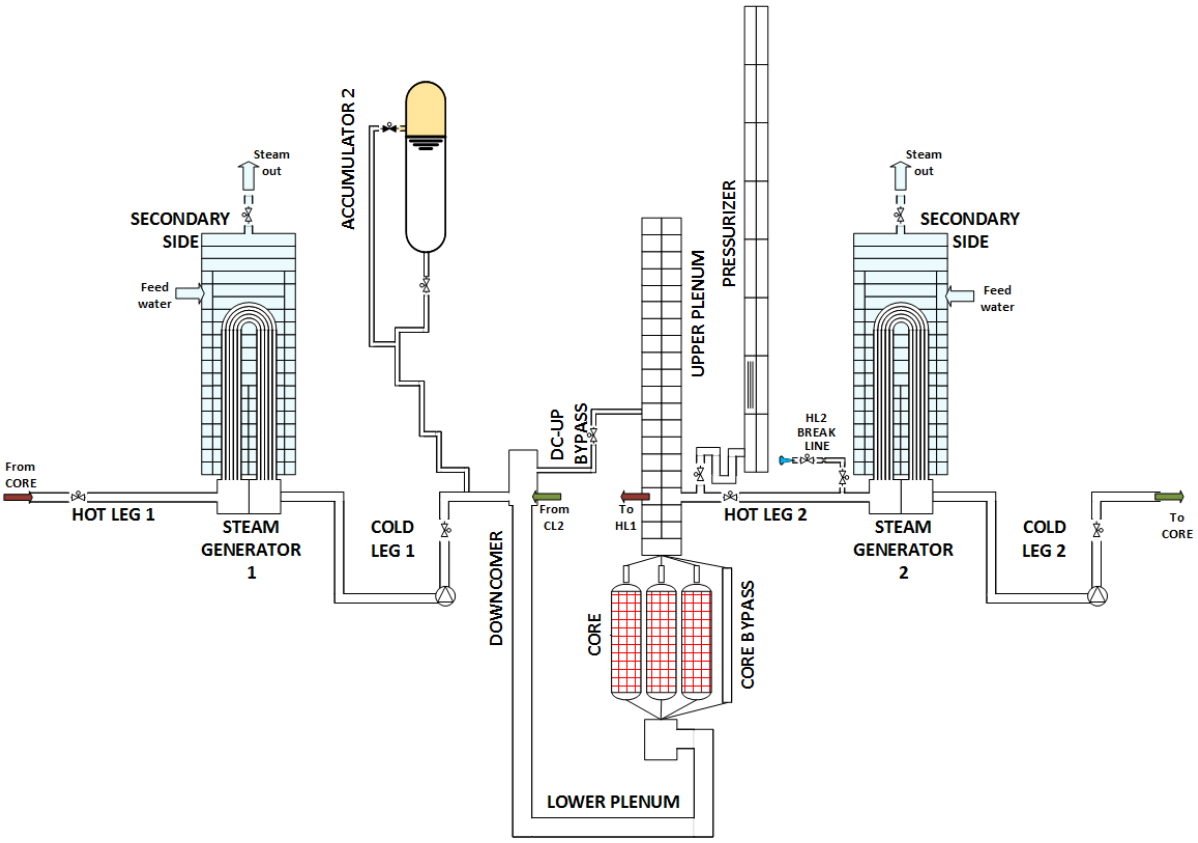

Fig. 3 Schematic diagram of the APROS nodalization.

The steam generators are modelled in the same manner in both nodalizations. The 51 heat exchange U-tubes of the PWR PACTEL steam generators are lumped together into five parallel pipe components in both models according to the different main lengths of the U-tubes. The hot and cold steam generator plenums are modelled with single nodes each. The secondary side nodalization of both steam generators includes the volumes of the hot and cold downcomer, riser, steam dome, and steam pipelines, as well as the pressure and feedwater control systems.

The accumulator and related piping are modelled in detail in both nodalizations, utilising code special features and options. The flow injection from the accumulator is controlled with pressure check valve models in the accumulator pipeline. In the TRACE nodalization, the accumulator is modelled with a pipe component using an accumulator modelling option available in the code. In the APROS nodalization, the accumulator is modelled with a heat tank module with the interfacial heat transfer efficiency parameter increased by a factor of about nine to get the accumulator draining right. The pressurizer is modelled with a single vertical pipe component in the TRACE nodalization. In the APROS nodalization, the pressurizer includes two parallel vertical nodal columns with horizontal flow connections, implemented to enhance the internal water circulation and temperature simulation.

The break line piping from the hot leg to the break orifice and from the orifice to the break valve is included in both nodalizations. In both nodalizations, the critical flow model is enabled at the break orifice. The calculation of the critical flow conditions is one of the important factors affecting the progression of the LOCA simulation. In both simulation models, the break line geometry was modelled with a relatively detailed including the break orifice plate and the following break valve. The form loss coefficients along the break line and the orifice plate in both simulation models and the discharge coefficient attribute for the break in the APROS model were adjusted to get a comparable break flow rate.

4. Procedure and general progression of the PWR PACTEL nitrogen experiment NCG-13

During the nitrogen experiment NCG-13, the accumulator injection was connected to the end part of the cold leg in the intact loop. The break location was on the top side of the hot leg in the broken loop, between the connection of the pressurizer surge line and the steam generator. The break was realized with a break line with an orifice plate. The break size was 5.5 mm, which is about 1.1 % of the PWR PACTEL cold leg cross-sectional area. The leaked water mass from the break line was collected and measured in a separate collector tank. A connection line with an orifice plate connected the downcomer top and the upper plenum middle parts (above the cold and hot leg connection level).

The experiment was performed under natural circulation conditions. First, a steady state operation at the full inventory was established. Then, the actual transient was started by opening the break. Table 1 presents the initial conditions at the beginning of the transient in the experiment. The secondary side water levels were maintained at initial values throughout the transient. The used safety functions were the accumulator water injection to the intact loop and the secondary side depressurization of both steam generators. The accumulator was initially pressurized with nitrogen to 45 bar. The secondary side depressurization started with the cooldown rate of 100 °C/h when the primary side pressure decreased below 43 bar.

A core protection system (CPS) was utilized to protect the facility from overheating. CPS was set to limit the core heat up by decreasing the core power when a threshold temperature value was reached. The experiment was terminated after CPS was initiated.

Table 1. Initial conditions in the NCG-13 experiment and simulations.

Experiment	NCG-13	TRACE	APROS
Primary side pressure	75.0 ± 0.4 bar	74.8 bar	74.4 bar
Secondary side pressure	40.0 ± 0.3 bar	40.1 bar	40.0 bar
Core power	150 ± 6 kW *	144 kW	144 kW
Total mass flow rate	1.1 ± 0.3 kg/s	1.0 kg/s	1.0 kg/s
Pressurizer water level	5.52 ± 0.14 m	5.50 m	5.51 m
SG collapsed level	3.9 ± 0.1 m	3.9 m	3.89 m
Core inlet temperature	246 ± 2 °C	246 °C	246 °C
Core outlet temperature	275 ± 2 °C	275 °C	276 °C
Feedwater temperature	25 ± 1 °C	25 °C	25 °C
Accumulator pressure	45.3 ± 0.4 bar	45.2 bar	45.2 bar
Accumulator temperature	51 ± 3 °C	51 °C	50 °C
Accumulator water level	1.31 ± 0.04 m	1.31 m	1.31 m

** The planned value was 150 kW; the averaged measured value was near 144 kW.*

The main results of the experiment are presented in Figs.Fig. 4-Fig. 10. As the break was opened and the leak from the primary system started (Fig. 4), the primary side pressure (Fig. 5) dropped sharply until the saturation temperature reached the core outlet temperature. The pressure decrease caused water in the core region to boil and water in the upper plenum to flash into steam. The increasing steam production slowed down the descending rate of the primary side pressure until the collapsed water level in the upper plenum decreased below the hot leg elevation (Fig. 6). This enabled more steam to flow through the hot legs into the steam generators and out of the break. The steam flow to the hot legs caused the primary side pressure to drop near the level of the secondary side pressure and the start of the accumulator water injection and the secondary side depressurization.

During the accumulator water injection period and the secondary side depressurization, the heat from the primary side was removed through the break and through the steam generators to the secondary side. The primary side and accumulator pressures followed the decreasing secondary side pressures (Fig. 5). Since the break was in the hot leg, steam produced in the core had a short and direct route to the break. The collapsed water levels on the pressure vessel core and downcomer sides were in a hydrostatic equilibrium determined by the acceleration due to boiling in the core (Fig. 6).

When the water injection from the accumulator ended, nitrogen from the accumulator was allowed to flow to the cold leg of the intact loop. The flow rate of nitrogen injection was controlled by the pressure difference between the accumulator and the primary system. During the nitrogen injection period, the primary side depressurization was halted (Fig. 5). At this point, also the nitrogen injection stopped, for lack of driving force. The primary side pressure stayed at the moderately constant level of 16.5 bar during the whole nitrogen injection period until the core heat up occurred. The water levels above the core and in the downcomer decreased due to boiling in the primary side and the mass inventory reduction through the break (Fig. 6), causing the core heat up at 3325 seconds after SOT. CPS started to decrease the core power at 3502 seconds after SOT when the core temperatures increased to high values, and finally the experiment was terminated.

5. Simulation results of the NCG-13 experiment

5.1 General progression of the simulations

In both simulations, the initial conditions at the beginning of the transient are well simulated (Table 1). The initial downcomer mass flow rates are slightly underestimated but are still inside the error limits of the measurement. The timings of the main events in the experiment and the simulations are presented in Table 2. In Figs.Fig. 4-Fig. 13, Fig. 15, and Fig. 17, the timings in the experiment and in some cases in the simulations are presented with vertical lines.

Table 2. Times of the main events in the NCG-13 experiment and simulations.

Experiment	Abbreviation *	Experiment	TRACE	APROS
Start of the transient	SOT	0 s	0 s	0 s
Accumulator water injection begins	ACC_W	450 s	404 s	424 s
Secondary side depressurization begins	SDE	495 s	449 s	450 s
Accumulator water injection ends and N_2 injection begins	ACC_W END	2278 s	2283 s	2254 s
Core heat up begins	HU	3325 s	3484 s	3206 s
Core protection system begins	CPS	3502 s	3653 s	3352 s

** Abbreviations used in figures from Fig. 4 onwards, pointing to times in the experiment.*

Fig. 4 presents the leaked mass from the primary system in the experiment and simulations. In the experiment, the leak mass flow rate is highest in the beginning of the transient. When the steam content in the leak flow increases before and after the accumulator water injection period, the leak flow rate decreases (the slope of the leaked water mass curve in Fig. 4 decreases). The general trend of the leaked mass with both codes corresponds relatively well with the experiment result although there are under- and overestimations along the transient. APROS overestimates the leak flow rate in the end of the accumulator water injection period and TRACE during the accumulator nitrogen injection period. These discrepancies in the simulations result from the different composition of the leak flow compared to the measured value. The proportions of water and steam in the leaked flow are different from the experiment and each other along the transient due to the different conditions (e.g. void fraction) in the hot leg at the break location. Also, the different modelling of the leak flow void fraction dependence on the hot leg conditions might have an effect to the different leak flow rate between the codes. However, the magnitude of this effect is difficult to estimate. At the end of the accumulator water injection period, the leaked mass in the TRACE simulation is underestimated approximately 1.2 % and in the APROS simulation overestimated approximately 3.9 %. At the time when CPS in the simulations is initiated, TRACE and APROS overestimate the leaked water mass approximately 4.1 % and 0.9 %, respectively.

Fig. 4 also presents the accumulator water mass injected to the primary side. The simulations show the trend of the injected water mass be comparable to the experiment. In the TRACE simulation, the accumulator water flow to the primary side is slightly underestimated during the middle part of the accumulator water injection period. The amount of the water injected into the facility at the time when the accumulator water injection period ends is about the same in the experiment and both simulations.

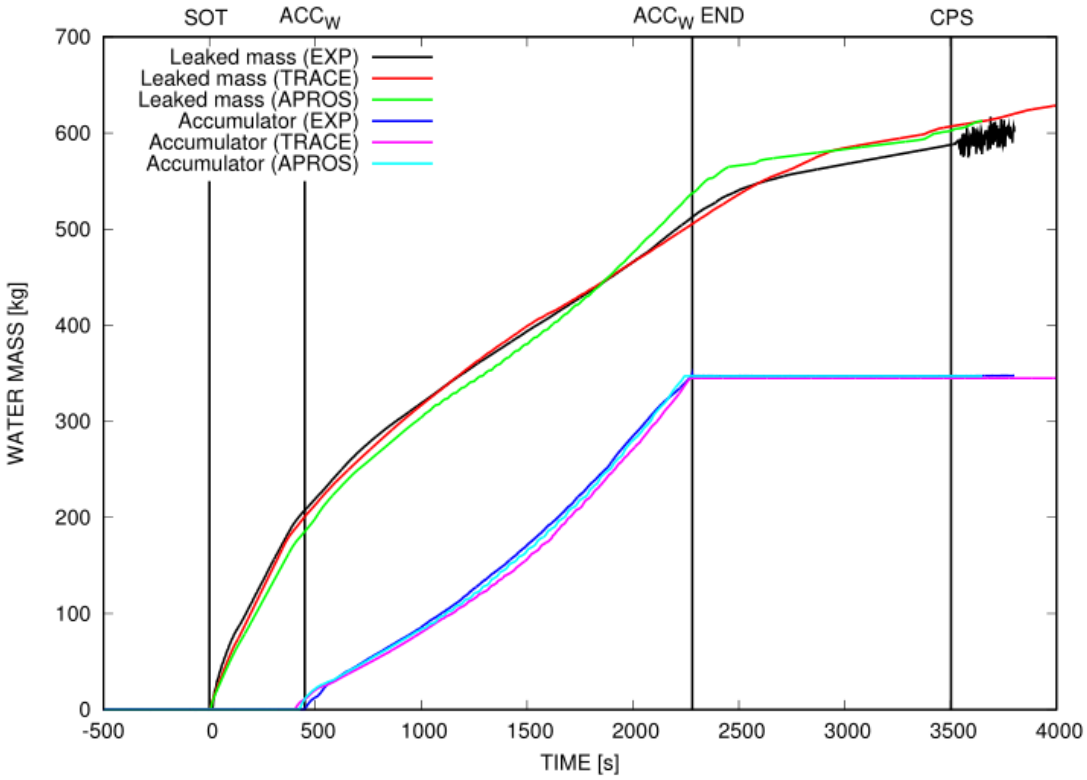

Fig. 4 Leaked water mass through the break (error margin < 5 %) and cumulative water mass released from the accumulator to the primary system in the NCG-13 experiment and simulations.

The general trend of the system pressures is moderately well predicted with both codes during the whole transient (Fig. 5). The collapsed water levels on the core side of the pressure vessel decrease to the hot leg level a slightly faster in both simulations compared to the experiment (Fig. 6) at the beginning of the transient. This causes the primary side pressure decrease to the secondary side level and the start of the accumulator water injection and the secondary side depressurization to occur slightly earlier in both simulations compared to the experiment (Table 2). In both simulations, the primary side depressurization stops after the nitrogen is released to the primary side (Fig. 5). During the nitrogen injection period, the primary side and accumulator pressures in the simulations decrease approximately 1-1.5 bar lower than in the experiment; the issue is discussed more in Chapter 5.2.

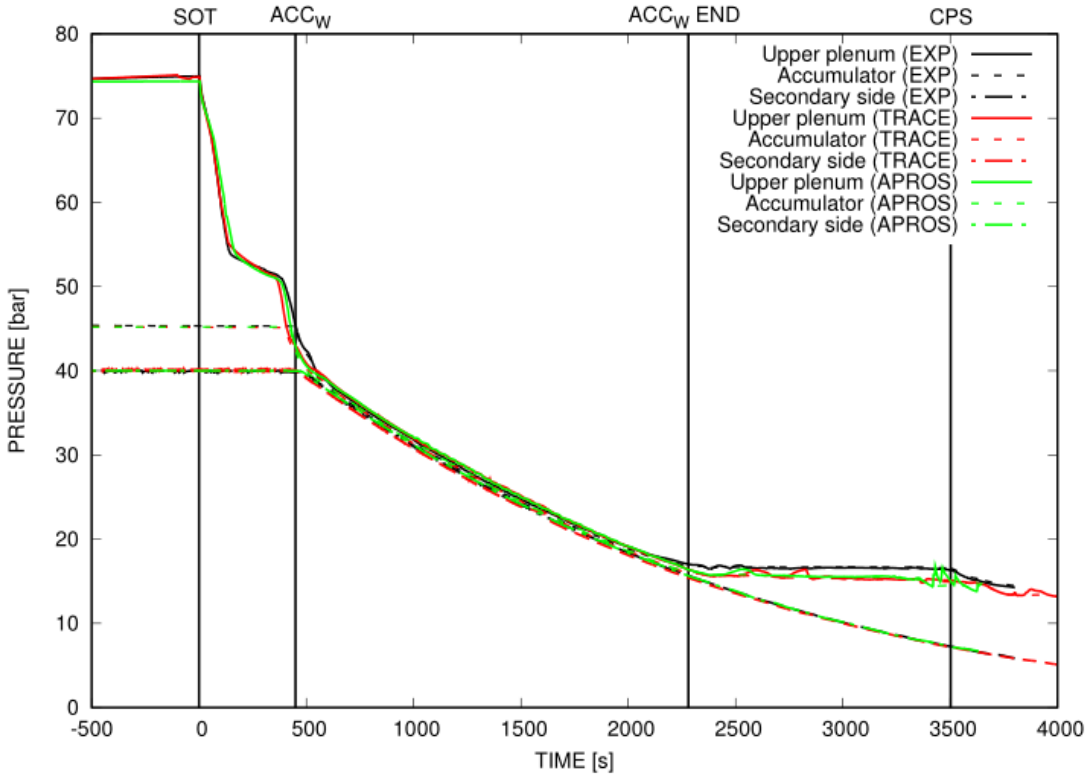

Fig. 5 Primary side, secondary side, and accumulator pressures in the NCG-13 experiment and simulations.

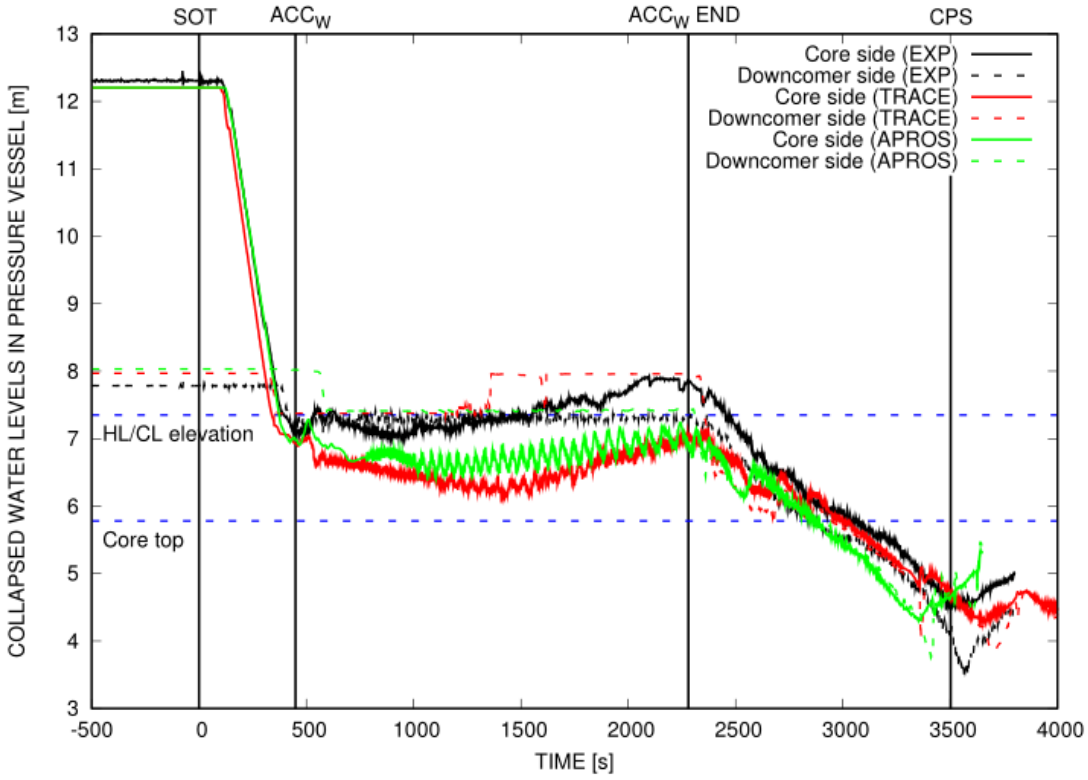

Fig. 6 Collapsed water levels on the core and downcomer side (error margins ±0.2 m and ±0.13 m, respectively) of the pressure vessel in the NCG-13 experiment and simulations.

During the accumulator water injection period, both codes underestimate the collapsed water level on the core side of the pressure vessel approximately 0.5-1.0 meters (Fig. 6). In the simulations, the water levels on the downcomer sides are at higher level than on the core side along the period. In the APROS simulation, the water on the downcomer side is at the level of the cold leg connections almost the whole accumulator water injection period, as in the experiment. In the TRACE simulation, the downcomer top fills up when the cold accumulator water condensates the steam volume in the downcomer top. As the filling occurs, the water levels on the cold sides of the steam generator U-tubes and on the core side decrease shortly.

The reason for the lower water levels on the core side of the pressure vessel could be that the codes do not predict the manometric balance of water in the primary system correctly, and water in the primary side is distributed differently in the simulations compared to the experiment. The pressure difference over the connection line orifice (Fig. 7) during the accumulator water injection period is positive in the experiment and simulations, meaning that the pressure in the upper plenum is higher than in the downcomer top and the flow direction through the connection line is towards the downcomer. However, in both simulations the pressure difference is overestimated. This can explain why in the simulations the water levels on the downcomer sides are at higher level than on the core side along the period (Fig. 6). The relatively higher pressure in the upper plenum can decrease the water level on the core side and push more water from the core to the downcomer and loops in the simulations compared to the experiment. In the experiment and simulations, both loop seals stay closed during the accumulator water injection period (Fig. 8). However, Fig. 8 shows the steam content on the downflow side of the loop seals in both cold legs in the experiment. Yet, in both simulations the oscillation on the water level is visible only on the downflow side of the loop seal of the intact loop. This indicates that the steam generators in the simulation model include more water than in the experiment; i.e. some of the water content that should be more on the core side of the pressure vessel is located in the steam generator volumes. From the experiment measurements, it is difficult to estimate the water amount in the steam generator plenums and U-tubes. In both simulations, both cold plenums are almost full of water during the accumulator water injection and there is also water in the cold side of the steam generator U-tubes.

Curves in Fig. 4 show that the water inventory in the primary side compared to the experiment situation during the accumulator water injection differs at times in both simulations. In the TRACE simulation, the water inventory is underestimated during the middle part of the accumulator water injection period due to lower accumulator water amount in the primary side. In the APROS simulation, the water inventory is slightly overestimated at the first part of the period and then underestimated at the end of the period due to the under- and overestimations in the leaked water mass. These differences can partly affect the water level on the core side.

At the beginning of the accumulator nitrogen injection period, the water levels on the core side of the pressure vessel are underestimated in both simulations approximately 0.8 meters. On the downcomer side, the water level is at the level of cold leg connections in the experiment and APROS simulation while in the TRACE simulation, the downcomer is full of water. During the accumulator nitrogen injection period, the water levels on the core and downcomer sides decrease in both simulations due to boiling and the mass inventory reduction, as in the experiment. In the TRACE simulation, the water level decrease is a bit slower, causing the core heat up to occur 159 seconds later than in the experiment (Table 2). In the APROS simulation, the water levels decrease is a bit faster than in the experiment, causing the core heat up to occur 119 seconds earlier than in the experiment.

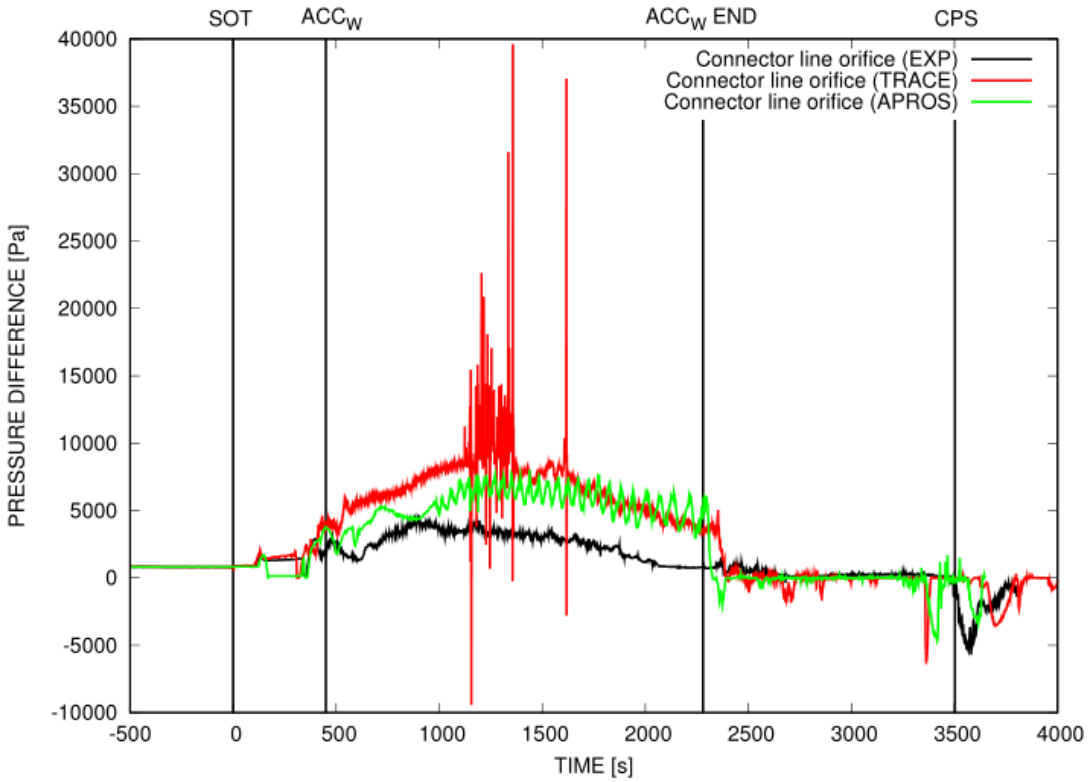

Fig. 7 Pressure difference over the connection line orifice in the NCG-13 experiment (error margin ±200 Pa) and simulations.

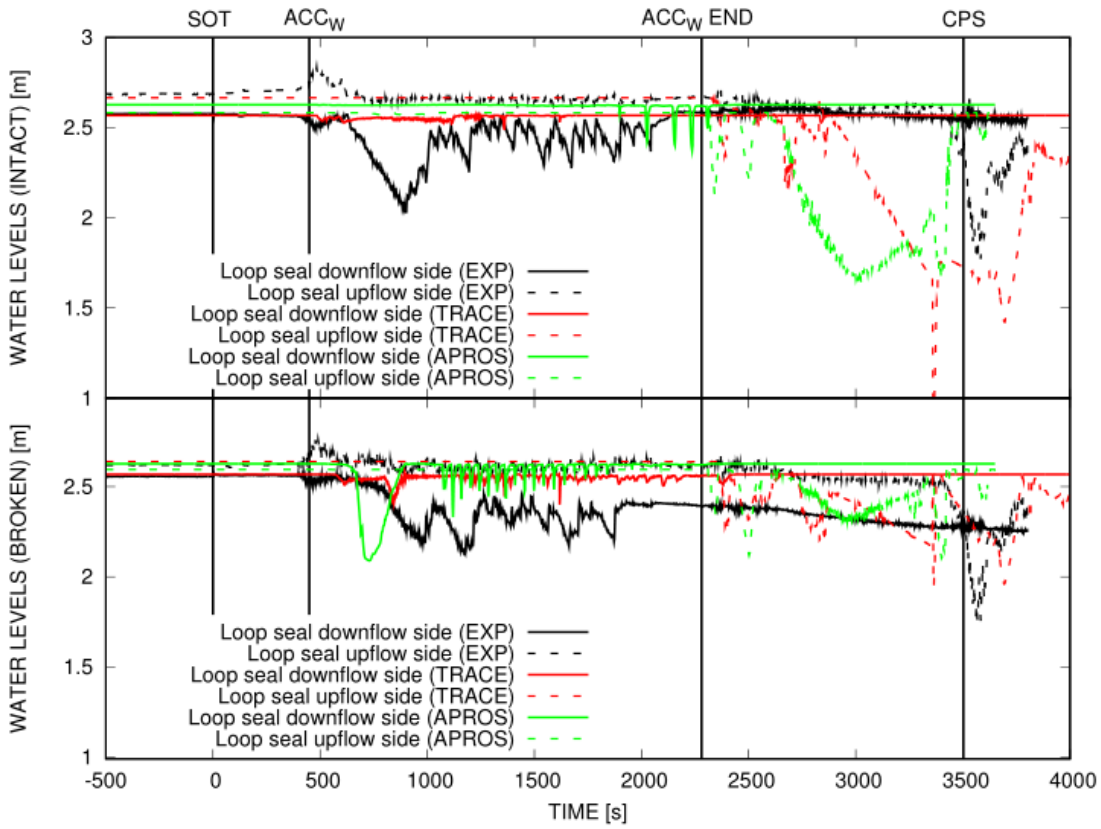

Fig. 8 Loop seal water levels in the NCG-13 experiment (error margins ±0.06 m) and simulations.

Fig. 9 presents the downcomer mass flow rate in the experiment and simulations. Both codes predict the downcomer mass flow rate well in the beginning of the transient. During the accumulator water injection, the downcomer mass flow rate starts to oscillate and it is underestimated in both simulations. In both simulations, the water flow through the intact loop decreases to near zero between 500 - 600 seconds after SOT when the water flow through the top of the steam generator U-tubes stagnates due to low water levels in the U-tubes. In the TRACE simulation, this stagnation lasts the whole accumulator water injection period while in the APROS simulation water starts to flow periodically through the U-tubes later in this period. In both simulations, the water flow in the broken loop starts to decrease first and then oscillate when the water periodically flows through the top of the steam generator U-tubes. The fluctuating behaviour causes the oscillation to the flow rate of the downcomer in the simulations. In the experiment, the downcomer flow rate stayed relatively stable during the accumulator water injection period, indicating the plausible continuous water flow through both loops. During the nitrogen injection period, the flow rates decrease to near zero values, visible in the simulations and apparently out of the range of the measurement device in the experiment.

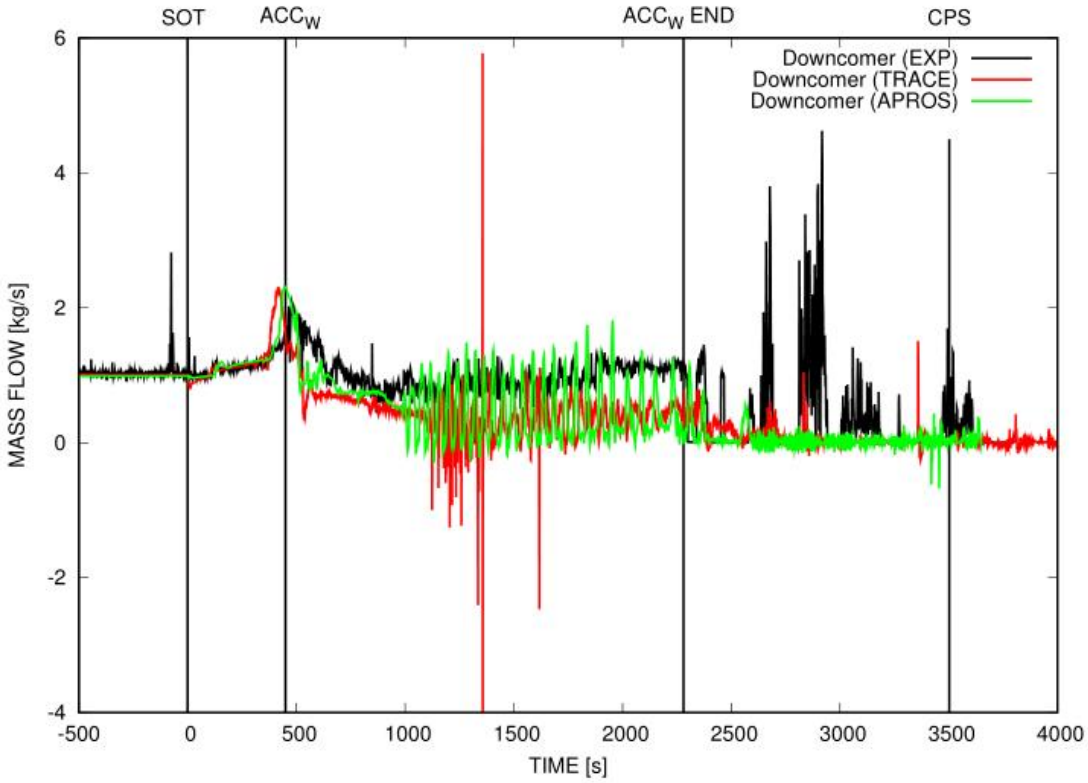

Fig. 9 Mass flow rate in the downcomer in the NCG-13 experiment (error margin ±0.3 kg/s) and simulations.

Fig. 10 presents the pressure vessel and loop seal bottom temperatures in the experiment and simulations. Before the accumulator water injection, both codes predict the temperatures well. During the accumulator water injection period, both codes predict low temperatures in the downcomer and below the core compared to the experiment. This results from the low mass flow through the loops. Due to the low mass flow through the loops, the proportion of the cold accumulator water in the downcomer is overestimated, causing the low temperatures in the downcomer. In the TRACE simulation, the part of the cold accumulator water flows also in the loop seal of the intact loop because the water flow through the steam generator U-tubes is stagnated, unlike in the experiment and APROS simulation. This decreases the loop seal bottom temperature well below the experiment value (Fig. 10). During the accumulator nitrogen injection, the temperatures in the downcomer and below the core increases since the cold accumulator water injection stops and the warmer water from the

loops flows into the downcomer. In the TRACE simulation, the temperatures in the downcomer and below the core remain at the low level because the cold accumulator water from the intact loop flows into the downcomer.

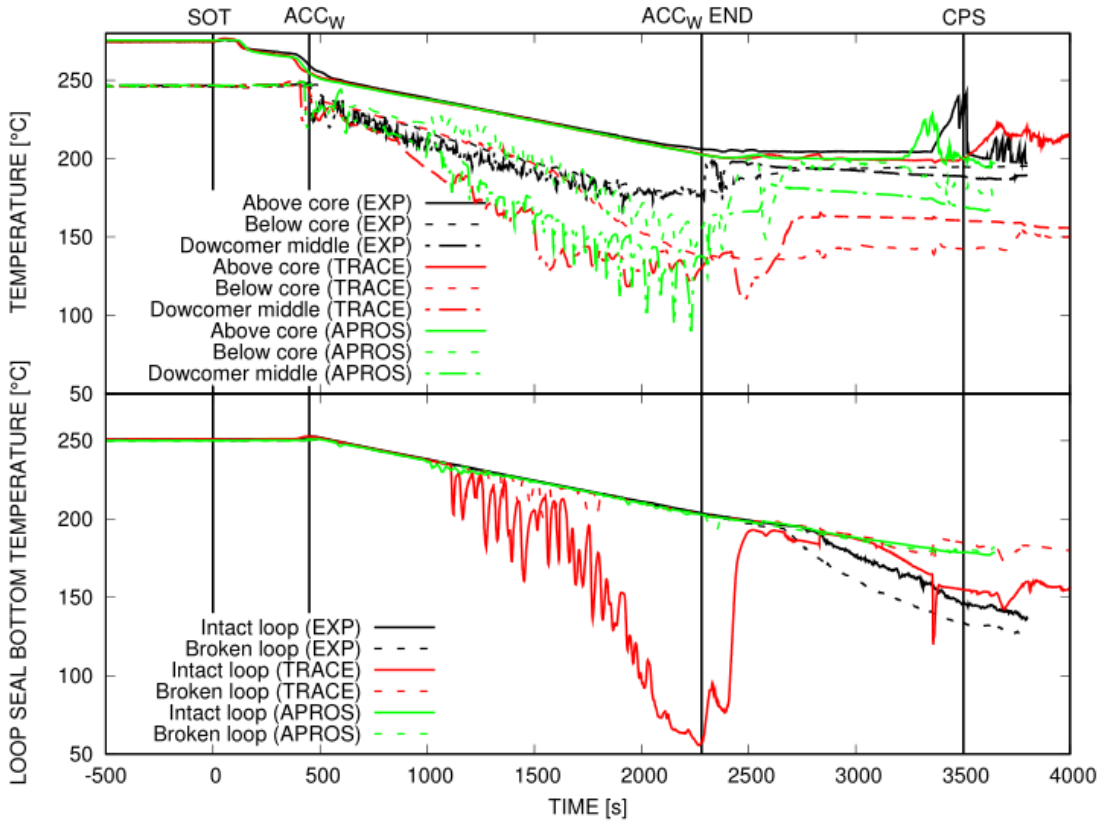

Fig. 10 Pressure vessel (top) and loop seal bottom (bottom) temperatures in the NCG-13 experiment and simulations.

5.2 The behaviour of the system pressures, water levels, and nitrogen migration during the nitrogen injection period

Due to the length of the accumulator line, it is impossible to tell the exact moment when the nitrogen started to enter from the accumulator line to the cold leg in the experiment. The time of the nitrogen valve opening is known but the accumulator line filling time is not. However, based on the primary side and accumulator pressures and the pressure difference over the orifice plate in the connection line, some estimates can be made on nitrogen arrival times and favourable periods for migration, presented in two top graphs in Fig. 11. At the beginning of the nitrogen injection period (ACC$_W$ END(EXP) in Fig. 11), the accumulator pressure decreased about 0.2 bar (Fig. 11, top graph, point A). Along this short period, nitrogen was released from the accumulator towards the primary side. The primary side depressurization was halted, though the upper plenum pressure experienced twice a short increase above and decrease below the accumulator pressure. At approximately 2550 seconds after SOT, the primary side pressure stabilized at a moderately constant level of about 16.5 bar. At periods when the primary pressure decrease stopped, based on the accumulator pressure measurement, it is impossible to estimate if more nitrogen was released from the accumulator. However, at these periods, the steep decreasing of the pressure difference over the connection line orifice (Fig. 11, middle graph) indicates a pressure increase in the downcomer top volume relative to the upper plenum. The pressure increase in the downcomer occurs due to the arrival and warm up of nitrogen in the downcomer top. The pressure difference showed also negative values, which is an indication on a reversal of the flow direction in the connection line (flow towards upper plenum). The reversal of the

flow direction allowed nitrogen to flow to the upper plenum and even further via hot legs to the steam generator U-tubes. In the U-tubes, steam condensed and nitrogen was enriched, blocking part of the heat transfer area and decreasing the condensation heat transfer.

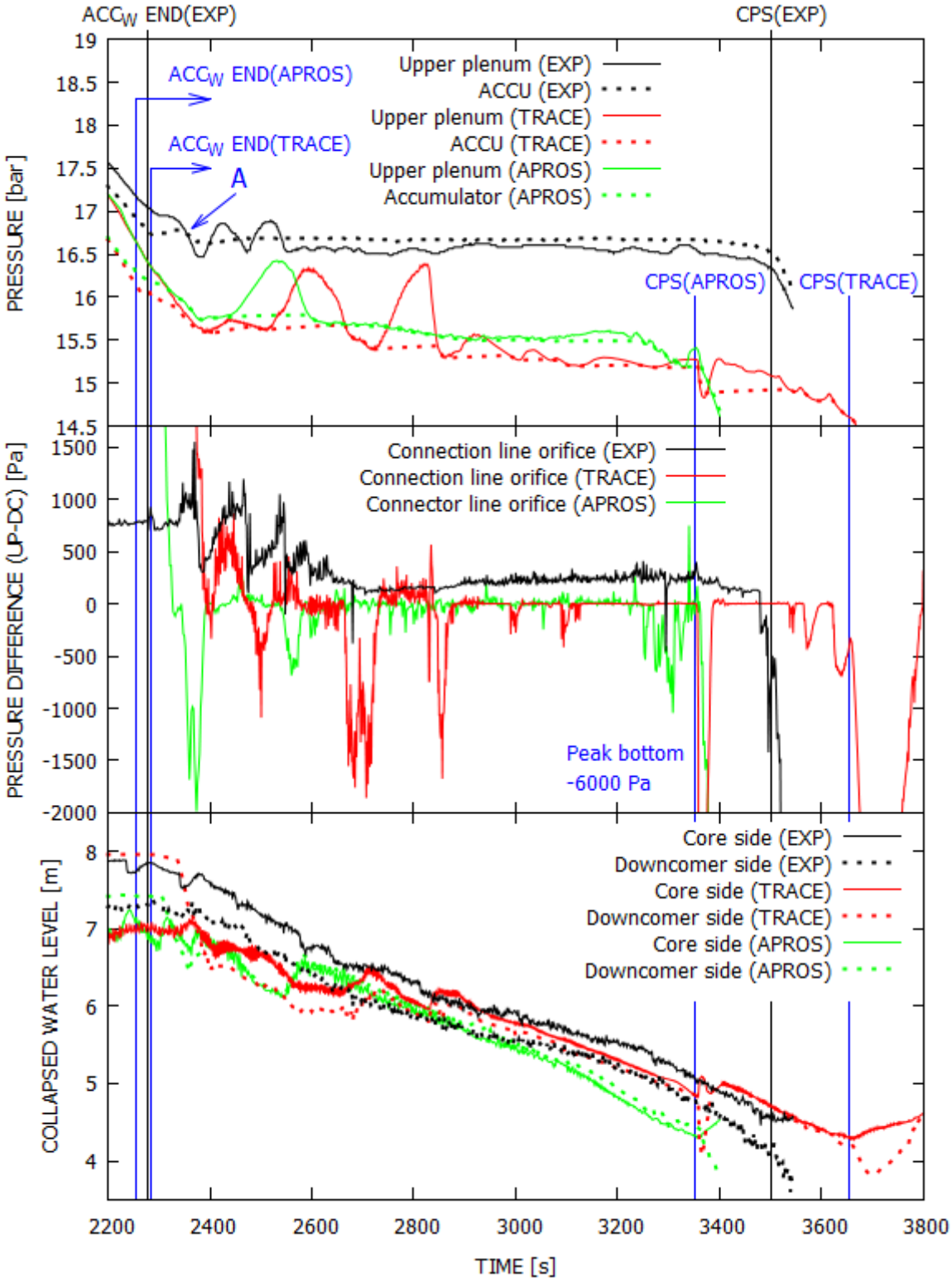

Fig. 11 Primary side and accumulator pressures (top), pressure difference over connector line orifice (middle), and collapsed water levels on the core and downcomer side of the pressure vessel (bottom) in the NCG-13 experiment and simulations. (A = accumulator pressure decrease, indicating nitrogen flow towards primary side in the experiment).

In the simulations at the end of the accumulator water injection period, the accumulator and primary side pressures are predicted approximately 0.5-1 bar lower compared to the experiment (Fig. 11, top graph). The lower pressure levels can result from the differences in the accumulator heat losses and the parameters that can affect the final nitrogen gas pressure in the accumulator after the accumulator water injection, such as the initial and final accumulator water levels and temperatures, and the initial pressure in the accumulator.

After the nitrogen injection begins in both simulations, the accumulator pressure decreases approximately 0.5 bar until the primary side depressurization ends, enabling the release of nitrogen from the accumulator. The accumulator injection pipeline is filled with water as the nitrogen injection starts. Hence, there is an approximately 50 seconds delay for the start of the nitrogen release to the primary side, as the nitrogen pushes the remaining water ahead before entering the cold leg. In both simulations, nitrogen starts to accumulate first in the downcomer top part (Fig. 12) where nitrogen displaces the water and decreases the downcomer water level (Fig. 11, bottom). Nitrogen increases the pressure in the downcomer top relative to the upper plenum and changes the flow direction in the connection line, allowing nitrogen to flow to the upper plenum. When nitrogen migrates from the downcomer to the upper plenum and forward to the hot legs and the steam generators, the primary side depressurization stops and the upper plenum pressure increases. In the TRACE simulation, nitrogen flows at first mostly to the steam generator of the intact loop and out through the break located in the hot leg of the broken loop, while nitrogen amount in the steam generator of the broken loop is much lower. In the APROS simulation, nitrogen flows in both steam generators and out through the break after it reaches the upper plenum.

In both simulations, the primary side pressure drops below the accumulator pressure after the primary side depressurization ends at the first time (Fig. 11, top), decreasing the accumulator pressure and releasing more nitrogen into the primary side (Fig. 12). The primary side pressure drop occurs because the steam/nitrogen mixture flows out through the break and/or pushes water through the loops to the downcomer. This water flow through the loops temporarily increases the water levels on the core and downcomer side of the pressure vessel (Fig. 11, bottom), delaying the core heat up. The released nitrogen increases the pressure in the downcomer top relative to the upper plenum, letting more nitrogen to flow to the upper plenum and the steam generator U-tubes, again stopping the primary side depressurization. The pressure increase and decrease appear in steps, gradually decreasing along the accumulator pressure. Fig. 12 also shows that in the simulations nitrogen in the primary side accumulates in the downcomer top parts and in the steam generator U-tubes but not in the upper plenum since nitrogen is heavier than steam and able to flow to the hot legs. In both simulations, the nitrogen amount in the pressurizer and the surge line is nearly zero during the whole transient.

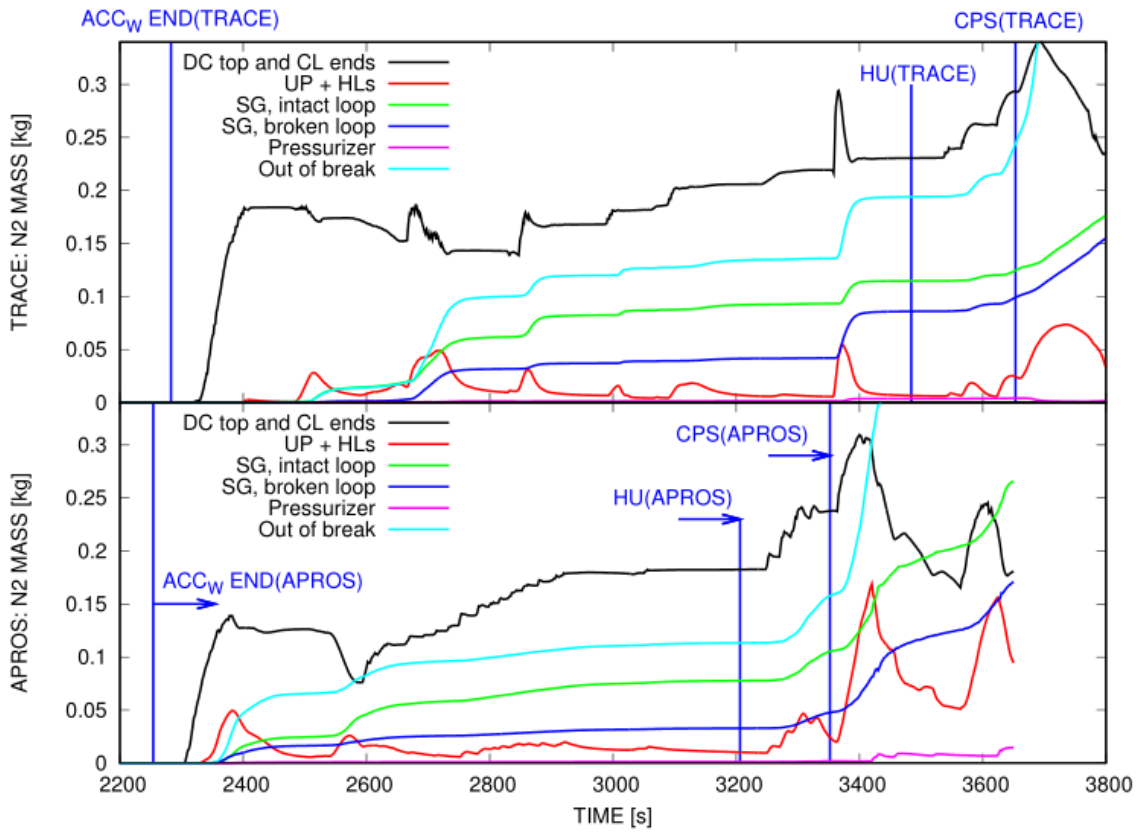

Fig. 12 Nitrogen masses in the different parts of the primary system during the nitrogen injection period in the TRACE (top) and APROS (bottom) simulation.

Fig. 13 presents the nitrogen masses released from the accumulator during the nitrogen injection period in the experiment and simulations. In the experiment, by using the ideal gas law, the estimated nitrogen content in the accumulator at the beginning of the transient was about 9.3 kg as calculated also in the simulations. Based on the accumulator pressure and temperature readings of the experiment, less than 150 grams of nitrogen was released from the accumulator before the core heat up occurred. This nitrogen amount was able to stop the primary side depressurization and keep the primary side pressure at a moderately constant level until the core heat up occurred.

In both simulations, substantially more nitrogen is needed to stop the primary side depressurization compared to the value evaluated for the experiment. In the simulations, the accumulator pressure decreases more during the nitrogen injection period compared to the experiment (Fig. 11, top). Hence, the nitrogen amounts released from the accumulator are approximately 2.5 times higher in the simulations compared to the experiment (over 300 grams released) before the primary side depressurization stops the first time and approximately 4-6 times higher before the core heat up occurs.

It is difficult to say what is the exact reason for the high nitrogen amounts in the simulations needed to stop the primary side depressurization. In the early post-test simulations, the interfacial heat transfer efficiency parameter of the accumulator in the APROS simulations, and the correlation constant value of the Wallis countercurrent flow limitation model (CCFL) at the ends of the steam generator U-tubes in the TRACE simulations were varied to predict the behaviour of the transient satisfactory (explained in more detail in Chapter 6). These parameter tunings in the models were relatively large and affected the accumulator draining, the pressure behaviour of the primary side and, consequently, the nitrogen release from the accumulator.

In the TRACE and APROS simulations, by the time when the core heat up occurs, the nitrogen amounts of 761 and 512 grams are released from the accumulator, respectively. Out of these, 75 % and 78 % are still inside the facility and the rest is leaked out through the break.

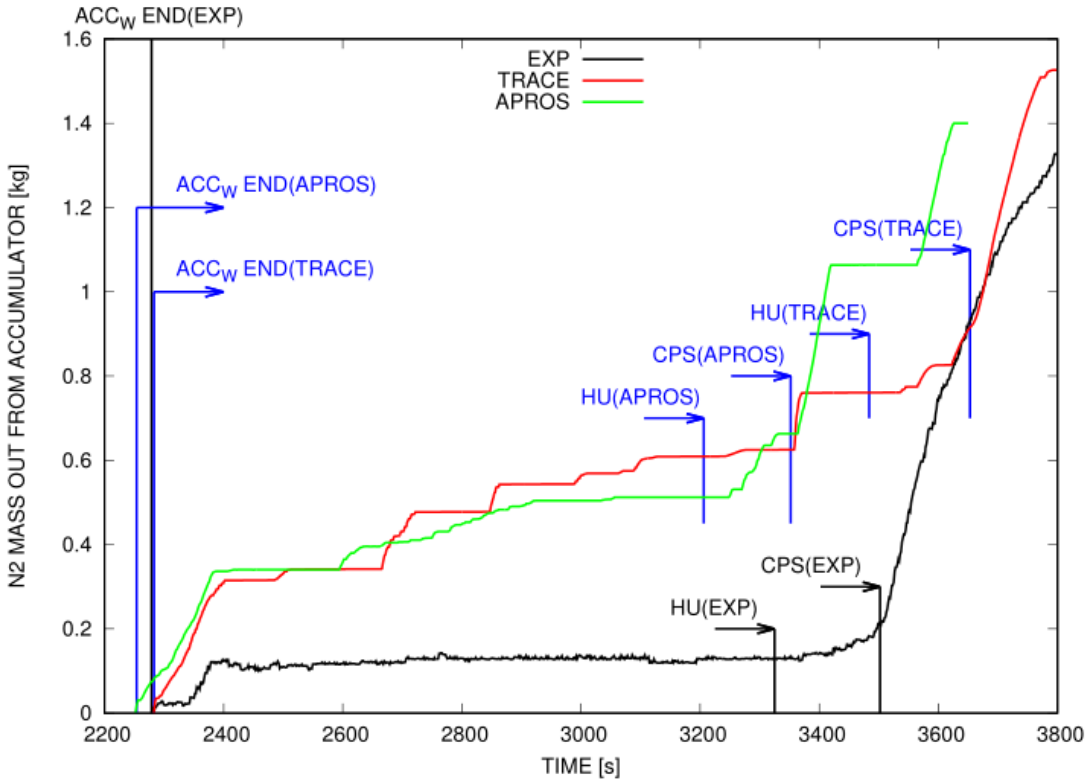

Fig. 13 Nitrogen mass out from the accumulator in the NCG-13 experiment and simulations.

Fig. 14 presents a still figure of the SNAP animation model of the TRACE nodalization, demonstrating the nitrogen and water inventory distributions in the primary system at the start of the core heat up. In Fig. 14 two animation models are presented side by side; one is animating node void fraction (white-blue colour map) and the other nitrogen gas density (white-red colour map). Fig. 14 shows that, as the core heat up starts, nitrogen in the primary side is divided in the downcomer top parts and in the steam generator U-tubes. According to Fig. 14, there is nitrogen also in the loop seal of the intact loop but the amount is small since the void fraction in those nodes is almost zero. Both loop seals are almost filled with water and there is still water in the steam generator U-tubes and plenums at the time when the core heat up starts (the same situation in the APROS simulation). The steam/nitrogen mixture in the upper plenum and hot legs opposes water to flow downwards from the hot side of the U-tubes. The steam/nitrogen mixture in the downcomer top keeps the loop seal water level below the elevation of the cold leg connection. During the accumulator nitrogen injection period, in the experiment, both loop seals were also closed (Fig. 8). However, from the available measurements, it is difficult to define how much water there was in the steam generator U-tubes. There are pressure difference measurements between the plenums and the U-tube top in six U-tubes in the steam generator of the broken loop in the facility. Fig. 15 shows the measured pressure differences for the short, middle, and long length U-tubes. These measurements indicate that there could be water content at least in some of the U-tubes during the nitrogen injection period.

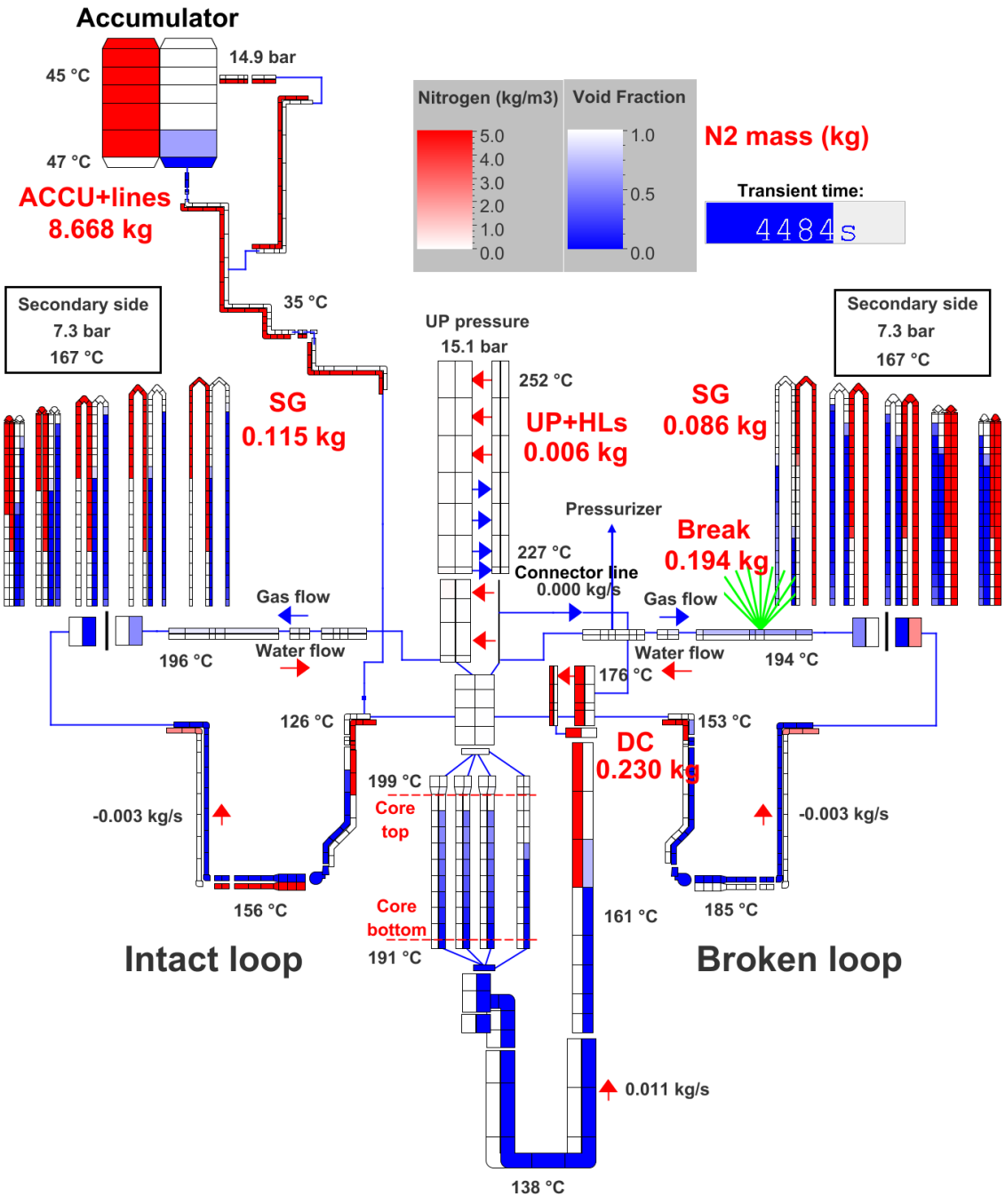

Fig. 14 Visualization of TRACE simulation at the start of the core heat up. Two models presented side by side: node void fractions with white-blue colour map, node nitrogen densities with white-red colour map. Nitrogen masses in different parts presented with red numbers.

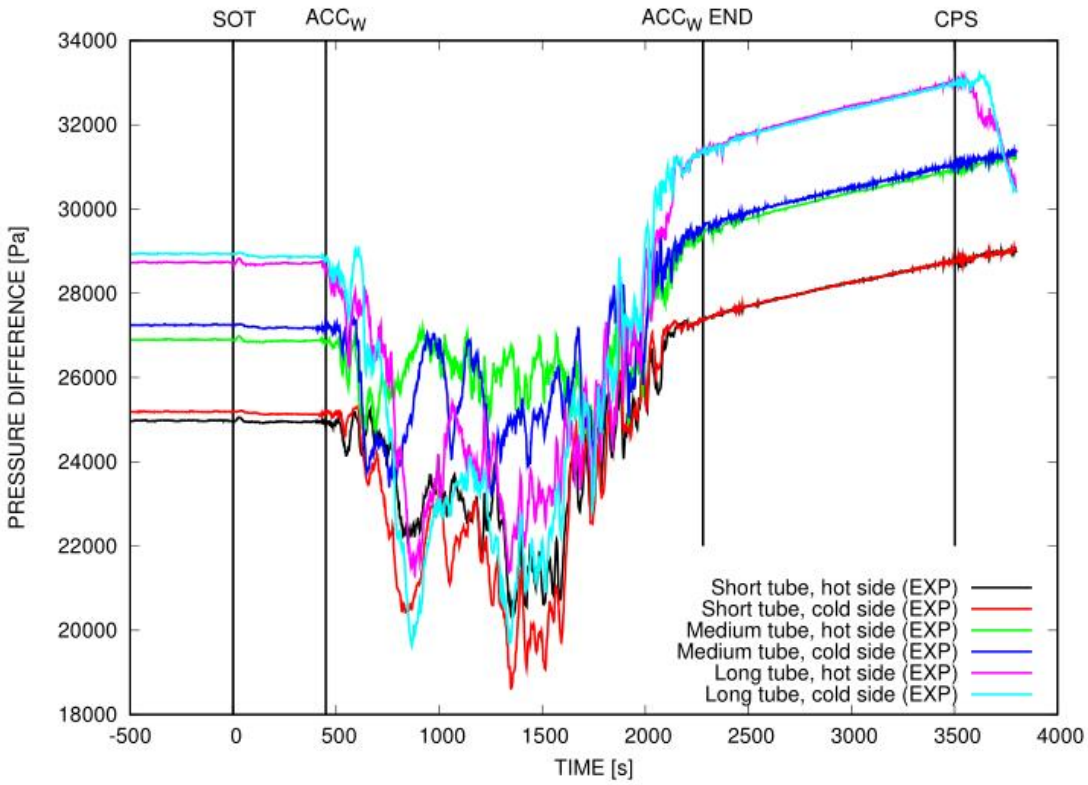

Fig. 15 Pressure difference between the plenums and U-tube top in the short, middle, and long height U-tubes of the steam generator of the broken loop in the NCG-13 experiment.

The nitrogen migration inside a steam generator heat exchange U-tube in the TRACE simulation is illustrated in Fig. 16. Two TRACE animation models are shown side by side (as in Fig. 14). In the figure, the nitrogen densities (left side tubes with the white-red color map) and void fractions (right side tubes with the white-blue color map) inside the middle height U-tube of the steam generator in the intact loop are presented at different times. In the simulation, the steam/nitrogen mixture starts to enter to the steam generator in the intact loop at approximately 2500 seconds after SOT. The steam condenses inside the U-tube, while the nitrogen flows through the condensate layer to the cold side of the U-tube. Nitrogen starts to accumulate on the U-tube cold side above the water level where it replaces the condensing steam and decreases the steam partial pressure. According to the TRACE simulation, the steam partial pressure decreases until it reaches the level of the secondary side pressure, and then starts to follow it. The steam condensation and heat transfer rate to the secondary side decreases substantially at this point. Because the total primary side pressure stays almost constant and the steam partial pressure decreases along the depressurization rate of the secondary side, the partial pressure of nitrogen increases steadily. When the nitrogen flow to the U-tube continues, nitrogen starts to occupy more space from the U-tube, filling up first the volume above the water levels in the top of the U-tube, and then the hot side of the U-tube. At 3484 seconds after SOT the core heat up occurs.

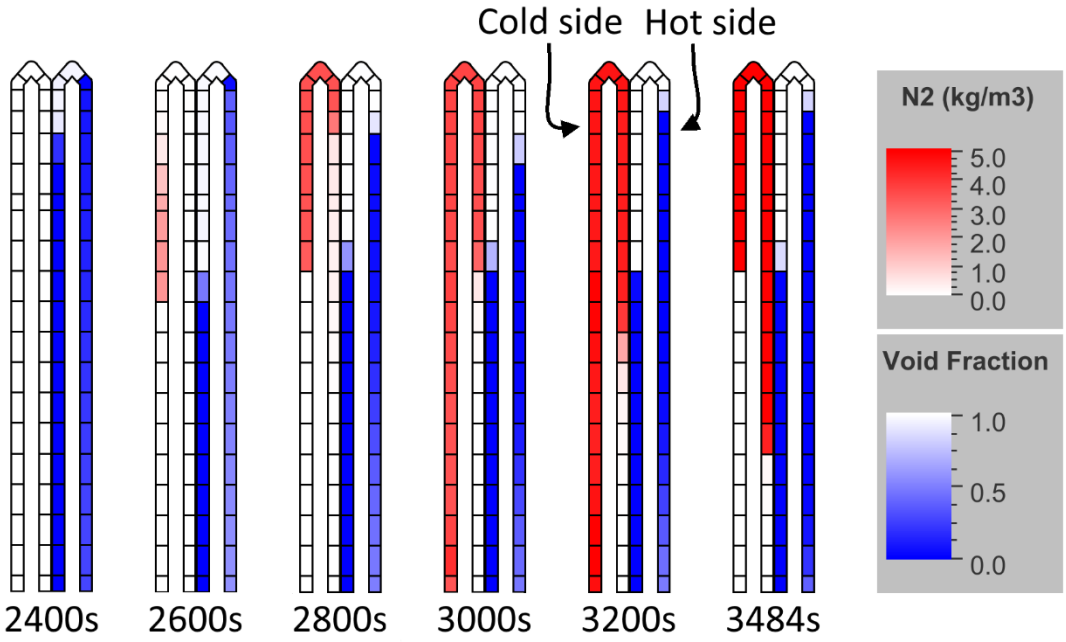

Fig. 16 Nitrogen migration in the middle height U-tube of the steam generator in the intact loop during nitrogen injection period in the TRACE simulation. Two TRACE animation models side by side: on the left side the node nitrogen densities presented with white-red colour map, on the right side the node void fractions with white-blue colour map.

In both simulation models, the 51 U-tubes of the PWR PACTEL steam generators were modelled with five parallel U-tube groups (lumped). The number of U-tube groups used in the steam generator model could have an influence on the calculation results and is discussed shortly in the SBLOCA benchmark exercise of PWR PACTEL (Kouhia et al., 2013). The benchmark exercise showed that using lower number of U-tube groups instead of the five parallel U-tube groups in the steam generator model the possible flow stagnation or reversal that took place during the transient cannot be captured in some of the U-tubes. The benchmark calculations implied that the simplified models with lower number of U-tube groups can predict the overall behaviour of the steam generator sufficiently enough, i.e. the loops flow rates and total heat transfer to the secondary side. In the transient discussed in this paper, the possible changes in the flow stagnation and reversal due to a lower number of U-tube groups could have an influence on the flow rate and oscillation in the downcomer during the accumulator water injection, and further to the temperature of the downcomer and core inlet. During the nitrogen injection period, the differences in the flow stagnation behaviour could have an effect on the water flow through the loops and possibly to the primary and accumulator pressure behaviour and the nitrogen release from the accumulator. However, the effect of the U-tube modelling to the calculation results was not tested in this work. The previously made models with the five parallel U-tube groups were decided to be used here as the models were considered to give a good prediction of the primary side mass flow rate and the behaviour and migration of nitrogen in the steam generator U-tubes in this transient.

6. Remarks of the TRACE and APROS post-test simulations

During the first post-test simulation tests with TRACE, the collapsed water level decrease in the pressure vessel was slower during the nitrogen injection period. The collapsed water levels on the core and downcomer sides decreased to the core top level and stabilized there for about 1000 seconds until started to decrease again. The stabilization resulted in the core heat up to occur 995 seconds later than in the experiment. The reason for the stabilization was the continuous water draining from the steam generator U-tubes of the intact loop and both cold legs to the core-downcomer section. The

draining water was able to compensate the boiling water mass. The water drained from the steam generator U-tubes of the broken loop was mainly discharged out from the break. When almost all the water from the steam generator U-tubes was drained and filled with nitrogen, the water level on the core side of the pressure vessel started to decrease and eventually led to core heat up. Timing of core heat-up in the experiment indicates that such water draining (reflux) did not occur in the experiment.

While building a TRACE nodalization, the user must define the CCFL model at the flow area restrictions, where the CCFL phenomenon is anticipated to occur (U.S. NRC, 2017). In the PWR PACTEL nodalization, the CCFL model is specified in two locations: at the choke plate above the core and at both ends of the steam generator U-tubes. During the first simulation tests, the Wallis CCFL model with the default correlation constant (C=1.0) and slope (m=1.0) values was used at the U-tube ends. In the latter simulation tests, a new correlation constant value for the Wallis CCFL model at the steam generator U-tube ends was chosen, to reduce calculated water draining from the steam generator U-tubes. The appropriate correlation constant value was calculated manually for the Wallis CCFL model, assuming that the water mass flow downward in the U-tubes is the same as the steam mass flow upward. The gas velocity and void fractions needed in these calculations were estimated from the previous simulation tests. These calculations estimated the correlation constant values between 0.15 and 0.3, depending on the used gas velocity and void fraction values (these values varied between the U-tubes). The correlation constant value of 0.2 gave the best fit to the experiment and was used in the TRACE simulation shown in this paper. The correlation slope default value was not changed. Fig. 17 shows the collapsed water levels in the pressure vessel on the core and downcomer sides as well as on the hot side of three steam generator U-tubes in both steam generators, before (default C=1.0) and after (C=0.2) the correlation constant change in the TRACE simulations.

In the APROS code the effect of the CCFL phenomenon is included in the calculation of the interfacial friction models. According to the code recommendations, for the core region in the APROS simulation model of PWR PACTEL, the alternative correlation fitting the particular rod bundle type was chosen. Otherwise, the default correlations for the interfacial friction calculation were utilized, without any modification in their parameters.

In APROS, the most notable tuning was made for the interfacial heat transfer efficiency parameter in the accumulator. The accumulator was modelled with a heat tank module with the efficiency parameter increased by a factor of about nine to get the accumulator draining right. The APROS hydroaccumulator model does not include wall heat transfer by default, it has to be modelled by the user separately. In early calculations, also APROS hydroaccumulator model was tested, and it needed the same increase of the efficiency parameter.

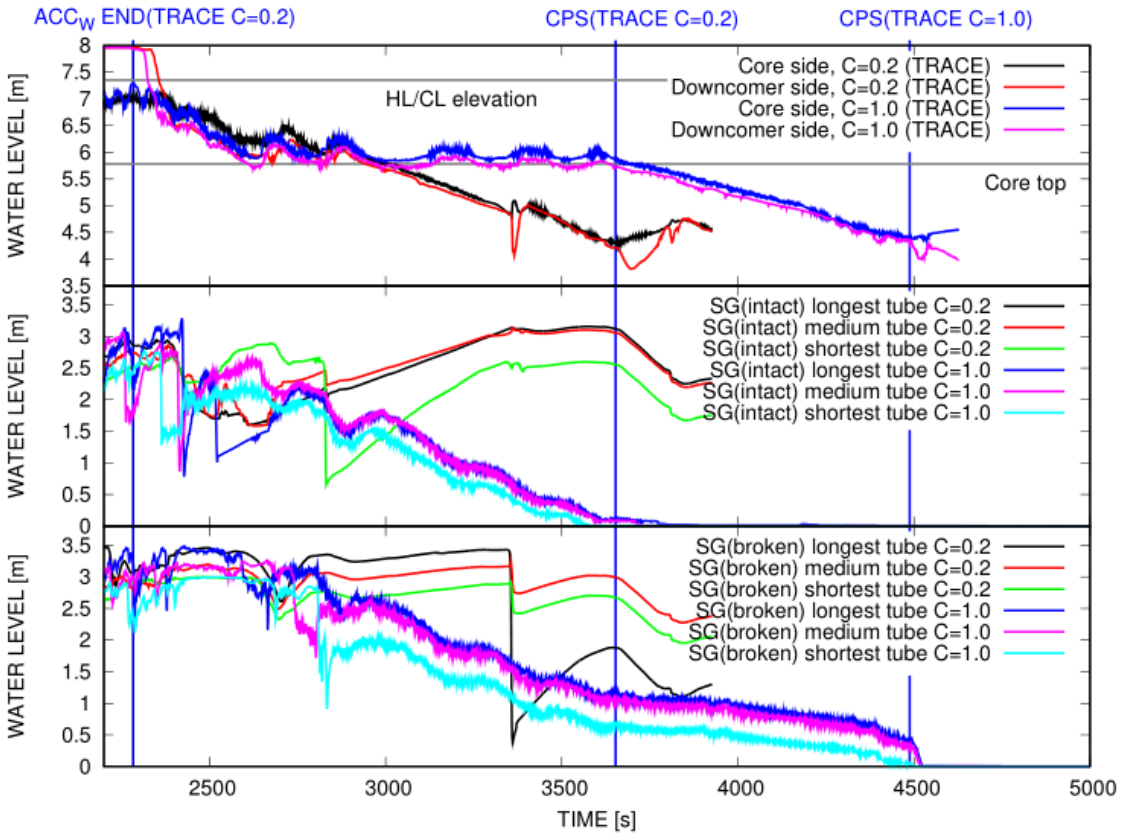

Fig. 17 Collapsed water levels in the pressure vessel (top) and in the hot side of three steam generator U-tubes in both steam generators (middle, bottom) during the nitrogen injection period in the TRACE simulations with different Wallis CCFL model correlation constants (C).

7. Conclusions

The PWR PACTEL nitrogen experiments included a hot leg LOCA situation with an accumulator nitrogen release into the primary side at the end part of the transient. The released nitrogen stopped the primary side depressurization during the secondary side depressurization and kept the primary side pressure constant until a core heat up occurred at a primary pressure above or very close to a typical low-pressure safety injection shut-off head. The objective of the analysis presented in this paper was to assess the capability of the TRACE and APROS system codes and nodalizations to predict the effects and migration of nitrogen in the primary side.

Both codes predicted the general behaviour of the transient and the timing of the main events, such as the initiation of the secondary side depressurization, the initiation of the accumulator water and nitrogen injection, and the beginning of the core heat up satisfactorily once suitable options of the code were chosen and adjustments could be made.

The primary side depressurization halted in the simulations when nitrogen reached the upper plenum and started to accumulate in the U-tubes. This halting is qualitatively correct, but the estimated amounts of nitrogen released from the accumulator were approximately 2.5 times higher in the simulations compared to experiments when the primary side depressurization stopped the first time, and approximately 4-6 times higher at the time of the core heat up. This difference is of concern regarding the confidence of the codes or the simulation models, because both codes clearly underestimate the adverse effect of nitrogen on core coolability.

In both simulations, during the accumulator nitrogen injection period, there was water in all steam generator U-tubes since the steam/nitrogen mixture in the upper plenum, hot legs, and downcomer top

prevented return of this water inventory into the core. In the TRACE simulation, the correlation constant value of the Wallis CCFL model at the U-tube ends had to be reduced significantly for the better prediction of the water draining from the U-tubes during the nitrogen injection period. Without the modification, water drained from the U-tubes to the core, delaying the core heat up substantially compared to the experiment. The correlation constant value was changed from the code default value of 1.0 to a value of 0.2. This value is presently justified only by the fact that it gives better fit of TRACE results to the experiment. Likewise, in the APROS modelling, the interfacial heat transfer efficiency parameter in the accumulator had to be tuned up by a factor of about nine, to get similar accumulator draining rate as in the experiment. It is noteworthy that using the code default parameters would lead to gross overestimate of the core heat up timing in both codes.

Acknowledgements

The Finnish Research Program on Nuclear Power Plant Safety 2015–2018 (SAFIR2018) and the Finnish power company Teollisuuden Voima Oy (TVO) have provided funding for the studies and analyses on the nitrogen experiments with the PWR PACTEL facility. The authors greatly acknowledge all the financiers of this research task.

References

Barbier, J.C, Clement, P.A., Deruaz, R.L., 1996. A hot leg break accident with HPIS failure and nitrogen injection by the accumulators in the BETHSY facility. International Conference on Nuclear Engineering (ICONE), volume 3, ASME 1996.

Hänninen, M., 2009. Phenomenological extensions to APROS six-equation model. Non-condensable gas, supercritical pressure, improved CCFL and reduced numerical diffusion for scalar transport calculation. Dissertation, Lappeenranta University of Technology. VTT Publications 720, VTT 2009. ISBN 978-951-38-7367-7.

Hänninen, M., Yli-Joki, J., 2008. The One-dimensional Separate Two-phase Flow Model of APROS. VTT Research Notes 2443, p. 65, VTT Technical Research Centre of Finland, Espoo 2008. ISBN 978-951-38-7224-3.

Kauppinen, O.-P., Kouhia, V., Riikonen, V., Hyvärinen, J., Sjövall, H., 2015. Computer analyses on loop seal clearing experiment at PWR PACTEL. Annals of Nuclear Energy, vol. 85, pp. 47–57. https://doi.org/10.1016/j.anucene.2015.04.036.

Kouhia, V., Purhonen, H., Riikonen, V., Puustinen, M., Kyrki-Rajamäki, R., Vihavainen, J., 2012. PACTEL and PWR PACTEL test facilities for versatile LWR applications. Integral test facilities and thermal–hydraulic system codes in nuclear safety analysis. Science and Technology of Nuclear Installations, vol. 2012, Article ID 548513, pp. 8. http://dx.doi.org/10.1155/2012/548513.

Kouhia, V., Riikonen, V., Kauppinen, O.-P., Purhonen, H., Austregesilo, H., Bánáti, J., Cherubini, M., D'Auria, F., Inkinen, P., Karppinen, I., Kral, P., Peltokorpi, L., Peltonen, J., Weber, S., 2013. Benchmark exercise on SBLOCA experiment of PWR PACTEL facility. Annals of Nuclear Energy, vol. 59, pp. 149–156. https://doi.org/10.1016/j.anucene.2013.04.004.

Kouhia, V., Riikonen, V., Partanen, H., Räsänen, A., Kauppinen, O.-P., Telkkä, J., Pyy, L., 2014. General description of the PWR PACTEL test facility, third edition. Technical Report, PAX 2/2014, Lappeenranta University of Technology, Nuclear Safety Research Unit. pp. 28 + 118 app. Lappeenranta.

Kral, P., Hyvärinen, J., Prosek, A., Guba, A., 2015. Sources and effect of non-condensable gases in reactor coolant system of LWR. The 16th International Topical Meeting on Nuclear Reactor Thermal-hydraulics, NURETH-16, Chicago, IL, August 30 - September 4, 2015. pp. 5194-5208.

Kurki, J., Ylijoki, J., Leskinen, J., 2019. APROS, The Constitutive Equations of the Two-Fluid Model. Apros version 6.09, May 2019. Apros 6, Reference manuals, Thermal hydraulics, Flow model 6, Constitutive equations. VTT Technical Research Centre of Finland.

Riikonen, V., Kouhia, V., Kauppinen, O.-P., 2016. PWR PACTEL nitrogen experiments. Research report, INTEGRA 1/2016, Lappeenranta University of Technology, Nuclear Engineering. pp. 23 + 17 app. Lappeenranta.

Riikonen, V., Kouhia, V., Kauppinen, O.-P., Hyvärinen, J., 2018. Experimental observation of adverse and beneficial effects of nitrogen on reactor core cooling. Nuclear Engineering and Design, vol. 332 (2018), pp. 111-118. https://doi.org/10.1016/j.nucengdes.2018.03.027.

Schollenberger, S. P., Umminger, K., Schoen, B., Dennhardt, L., 2017. PKL-ROSA/LSTF counterpart testing on beyond-design-basis SB-LOCA. The 17th International Topical Meeting on Nuclear Reactor Thermalhydraulics, NURETH-17, Xi'an, China, September 3-8, 2017.

Takeda, T., Ohtsu, I., 2018. Uncertainty analysis of ROSA/LSTF test by RELAP5 code and PKL counterpart test concerning PWR hot leg break LOCAs. Nuclear Engineering and Technology, vol. 50 (2018), pp. 829-841. https://doi.org/10.1016/j.net.2018.05.005.

U.S. NRC, 2017. TRACE V5.0 Patch 5 Theory manual. Field equations, Solution methods, and Physical Models. Division of safety Analysis, Office of Nuclear Regulatory Research, U.S. Nuclear Regulatory Commission, Washington, DC.